System Reliability Analysis Using Tail Modeling

Palaniappn Ramu[1], Nam H. Kim[2] and Raphael T. Haftka[3]
University of Florida, Gainesville, Florida, 32611

and

Nestor V. Queipo[4]
University of Zulia, Maracaibo, Venezuela

This paper presents an approach for system reliability analysis where a tail model is used for computing the reliability constraints. The tail model is an adaptation of a powerful result from extreme value theory in statistics related to the distribution of exceedances. The conditional excess distribution above a certain threshold is approximated using the generalized Pareto distribution (GPD). The shape and scale parameters in the GPD are estimated using either maximum likelihood or the least square method. The tail modeling technique is utilized to approximate the probability of failure in reliability analysis. The proposed method does not approximate the functional expression of the model output; rather approximates the tail of the cumulative distribution. Thus, it has an advantage of the system reliability analysis in which no single form of functional expression is available. The effectiveness and efficiency of the proposed approach are demonstrated using benchmark problems in structural design with multiple performance measures.

I. Introduction

RELIABILITY analysis involving system performance has been challenging because traditional methods, such as moment-based methods and response surface methods, cannot evaluate the system reliability accurately when the correlation between multiple performance functions is unknown. In addition, Monte Carlo methods for these tasks often fail to meet constraints (computational resources, cost, time, etc.) because the relatively high number of simulations required for evaluating the reliability constraints typically present in industrial environments.

In reliability analysis, the interest lies in the occurrence of rather exceptional events (tail part of probability distribution). In that regard, the moment-based method and the response surface method are not suitable because they are focused on the central part of the probability distribution. It is generally accepted that using central models (e.g., response surfaces) for estimating large percentiles such as those required in reliability constraint calculations can lead to significant inaccuracies in the RBDO results (e.g., Maes and Huyse[1]).

This paper presents a reliability analysis approach with the system reliability constraint. The reliability constraint is computed from rather general tail models available from extreme value theory in statistics (Castillo[2]). The conditional excess distribution above a certain threshold is approximated using the generalized Pareto distribution (GPD). The parameters in GPD are calculated using either the maximum likelihood function or the least square method. By incorporating the tail modeling technique with the probability of failure, the reliability analysis can be carried out for a structure with the system reliability constraint. The proposed method does not approximate the functional expression of the performance function; rather approximates the tail of the cumulative distribution. Thus, it has an advantage of the system reliability analysis and design in which no single form of functional expression is available.

---

[1] Graduate Student, Dept. of Mechanical & Aerospace Engineering, AIAA Member.
[2] Assistant Professor, Dept. of Mechanical & Aerospace Engineering, AIAA Member.
[3] Distinguished Professor, Dept. of Mechanical & Aerospace Engineering, AIAA Fellow.
[4] Professor, Applied Computing Institute, Faculty of Engineering

The paper is structured as follows. In Section 2, the tail of the cumulative distribution function is modeled using the generalized Pareto distribution. The RBDO framework using the tail modeling technique is presented in Section 3. Two numerical examples are presented in Section 4, followed by conclusions in Section 5.

II. Tail Modeling and Generalized Pareto Distribution

The cumulative distribution of a random variable can be decomposed into three parts: a lower tail, a central part, and an upper tail. Identifying a probabilistic model for large (extreme) values of the random variable is a key for a more accurate evaluation of the reliability constraints. The extreme value theory in statistics can be used for this purpose, as it provides a powerful result related to the distribution of exceedances called generalized Pareto distribution (Pickands[3]) that can be adapted for solving reliability constraints.

The fundamental idea of the tail–modeling technique stems from the property of tail equivalence. Two distribution functions $F(x)$ and $G(x)$ are called *tail equivalent* (Maes and Breitung[4]) if

$$\lim_{x\to\infty}\frac{1-F(x)}{1-G(x)}=1 \tag{1}$$

As far as the extreme behaviors of the two distributions are equivalent, the tail–model of $F(x)$ can be used to approximate the upper (or lower) tail of $G(x)$. This approach does not take into account the central behavior of the distribution. Rather, it focuses on the tail behavior, which fits for the purpose of structural reliability analysis.

In reliability analysis of structural systems, the cumulative distribution of a performance function is the most important criterion to determine the safety of the system. Let $\mathbf{x}$ be the vector of input random variables. Due to the uncertainty propagation, the performance function, $y(\mathbf{x})$, also shows random distribution. Let the performance function, $y(\mathbf{x})$, be a random variable and g be a large threshold of y (see Figure 1). For the region that y is greater than g, the GPD represents a general approximation of the conditional excess distribution $F_g(z)$ where $z=y-g$; that is, the distribution of values of a random variable y above a certain threshold g. Specifically, a theorem from extreme value theory establishes that for large values of g, $F_g(z)$ can be well approximated by:

$$F_g(z)\approx \hat{F}_{\xi,\sigma}(z), \tag{2}$$

where

$$\hat{F}_{\xi,\sigma}(z)=\begin{cases}1-\left\langle 1+\dfrac{\xi}{\sigma}z\right\rangle_+^{-\frac{1}{\xi}} & \text{if } \xi\neq 0\\ 1-\exp\left(-\dfrac{z}{\sigma}\right) & \text{if } \xi=0\end{cases}. \tag{3}$$

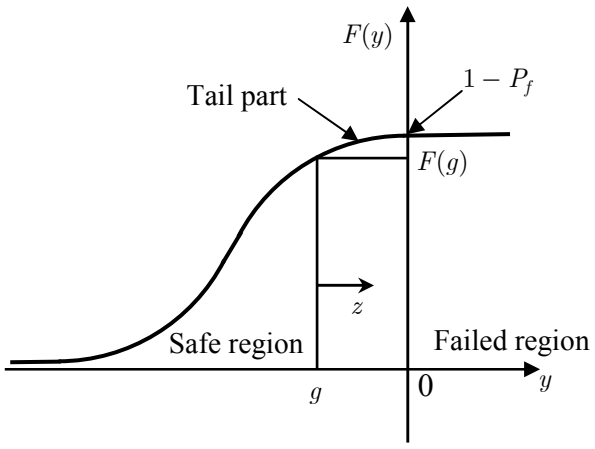

Figure 1: Tail–modeling of $F(y)$ using the threshold value of g.

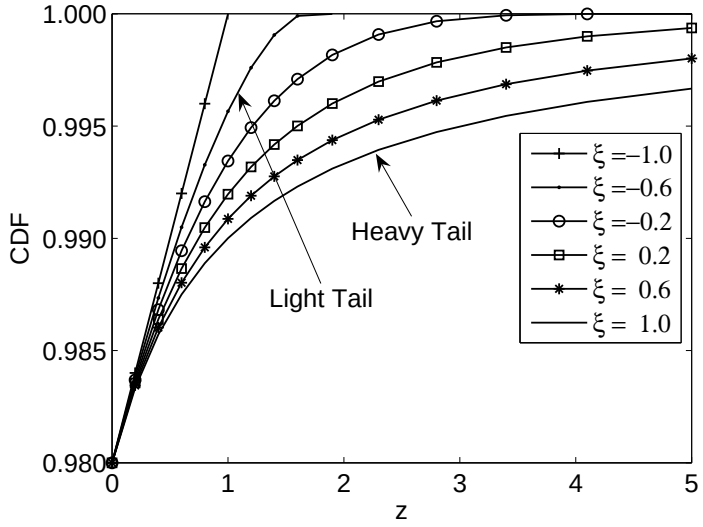

Figure 2: Generalized Pareto distributions for different shape parameters

In Eq. (3), $\langle A \rangle_+ = \max(0, A)$ and $z \geq 0$. $\hat{F}_{\xi,\sigma}(z)$ in Eq. (3) is called the generalized Pareto distribution (GPD), and ξ and σ are the shape and scale parameters, respectively, which need to be determined.

Note that the conditional excess distribution $F_g(z)$ is related to the cumulative distribution of interest $F(y)$ through the following expression:

$$F_g(z) = \frac{F(y) - F(g)}{1 - F(g)}. \tag{4}$$

The flexibility of the GPD in Eq. (3) can be examined by changing its parameters and plotting the distribution above the threshold. Figure 2 shows the different cumulative distributions that are generated from the GPD when the scale parameter, σ, is fixed to one, and the threshold, g, is selected such that $F(g) = 0.98$. When the shape parameter $\xi > 0$, it represents the heavy tail behavior, such as Pareto distribution. On the other hand, when $\xi < 0$, it represents the light tail behavior, such as the beta distribution. Note that the uniform distribution can also be modeled using $\xi = -1$.

The appropriate value for g, that is, the specification of the beginning of the upper tail, has been the subject of extensive research, and empirical values for it has been proposed (e.g., Boos[5]; Hasofer[6]; Caers and Maes[7]). In Hasofer's study, for example, the use of $N_g \approx 1.5\sqrt{N}$ is suggested where N_g is the number of tail data and N is the total number of data. On the other hand, the shape and scale parameters in the GPD can be estimated using either maximum likelihood (Prescott and Walden[8]; Hosking[9]) or least-square method.

In general, two sources of errors are involved in tail–modeling: (a) lack of modeling capability, and (b) errors in random sampling and in the empirical CDF. The former is related to the flexibility of the tail–model in representing various tail behaviors, and the latter is related to the number of samples and to the appropriate selection the threshold. The effects of these two sources of errors will be discussed in the numerical examples.

III. Reliability Analysis Using Tail–Modeling

Reliability analysis in structural problems often means the evaluation of the probability of failure. In this section, the tail–model will be used to calculate the probability of failure analytically. In addition, the inverse reliability analysis can easily be performed because the analytical expression of the reliability is available. The accuracy and convergence of the tail–model will be discussed using various distribution types.

A. Probability of Failure

In structural reliability analysis, the probability of failure, P_f, is often used as a constraint, so that it should be less than the prescribed target probability of failure, $P_{f,\text{target}}$. An analytical expression for the constraint value is

now developed in three steps based on the GPD approximation and the available data. First, an explicit expression for $F(y)$ is obtained from Eq. (4), as

$$F(y) = [1 - F(g)]F_g(z) + F(g)\,. \tag{5}$$

Second, in the above expression $F_g(z)$ is substituted by the corresponding GPD in Eq. (3), and for the prescribed $F(g)$, the threshold is interpolated using

$$g = y_{j-1} + (y_j - y_{j-1})\frac{F(g) - p_{j-1}}{p_j - p_{j-1}}\,, \tag{6}$$

where p_j is the empirical CDF. After the substitutions, $F(y)$ can be written as

$$F(y) = 1 - (1 - F(g))\left\langle 1 + \frac{\xi}{\sigma}(y - g)\right\rangle_+^{-\frac{1}{\xi}}. \tag{7}$$

When the performance function, y, is defined such that the structural system is failed when $y > 0$ and safe when $y \le 0$, the probability of failure can be written as

$$P_f \coloneqq 1 - F(y = 0) = (1 - F(g))\left\langle 1 - \frac{\xi}{\sigma}g)\right\rangle_+^{-\frac{1}{\xi}}. \tag{8}$$

Equation (8) provides an analytical expression of the probability of failure, which can be directly used in evaluating the constraints in RBDO.

The estimation of the probability of failure in Eq. (8) is only valid when the threshold $g < 0$, which means that $P_f < 1 - F(g)$. Equivalently, the limit state $(y = 0)$ must belong to the tail part. When the safety margin of the structural system is small, the probability of failure does not belong to the tail part, and the above formula cannot be used for estimating the probability of failure. The requirement of the structural safety is usually given in the range of small probability of failure so that the above requirement is satisfied. During the process of design optimization, however, it may be possible that a design may produce a relatively unsafe configuration. In such a case, a special treatment is required to estimate the probability of failure below the threshold. However, the estimation does not have to be accurate because it is not the final design.

B. Reliability Index and Inverse Reliability Analysis

In reliability–based design optimization, two methods are often referred: the reliability index approach and the performance measure approach, or often called the inverse measure approach. An inverse measure is the value of the performance function that corresponds to the given value of the probability, while a reliability index is the index of the standard normal distribution, corresponding to the specific value of the performance function. These two approaches work well with the first–order reliability method (FORM), where the performance function is assumed to be normally distributed after linearization.

For the estimated probability of failure in Eq. (8), the reliability index, β, can be calculated using

$$\beta = -\Phi^{-1}(P_f)\,, \tag{9}$$

where $\Phi(\bullet)$ is the CDF of the standard normal random variable. The reliability constraint is then imposed using the reliability index, as

$$\beta \ge \beta_{\text{target}} \coloneqq -\Phi^{-1}(P_{f,\text{target}})\,, \tag{10}$$

where β_{target} is the target reliability index that corresponds to the target probability of failure, $P_{f,\text{target}}$.

On the other hand, the inverse measure approach calculates the value of the performance function, y^*, corresponding to the target probability of failure. Using tail–modeling in Eq. (8) with $P_f = P_{f,\text{target}}$, the inverse measure can be obtained by

$$y^*(\sigma,\xi) = g + \frac{\sigma}{\xi}\left[\left(\frac{P_{f,\text{target}}}{1-F(g)}\right)^{-\xi} - 1\right]. \tag{11}$$

The reliability constraint is then imposed using the performance function as

$$y^* \le 0\,. \tag{12}$$

When the tail is heavy, i.e., $\xi > 0$, the above formula can be used to find the value of the performance function $y^* (\ge g)$ that has probability of failure P_f. On the other hand, when the tail is light, i.e., $\xi < 0$, the value of the performance function can be found up to $y^* = g - \sigma/\xi$, at which $P_f = 0$.

In the literature (Lee *et al*.[10]; Youn *et al*.[11]), it has been presented that the inverse measure approach is more stable than the reliability index approach. When the probability of failure is zero, the latter shows a singularity. The difficulty in the reliability index approach is related to the transformation in Eq. (9). The reliability index approaches to the value of infinity as the probability of failure is reduced. Thus, it is difficult to calculate the reliability index when the target reliability is far from the failure surface. On the other hand, the inverse reliability analysis always yields a finite value of performance function that satisfies the target reliability. Ramu *et al*.[12] presented an inverse measure, called probabilistic sufficiency factor (PSF), when sampling–based methods are used.

The inverse measure used here is the probabilistic sufficiency factor (PSF) introduced by Qu and Haftka[16]. PSF is a safety factor with respect to the target probability of failure and hence combines the concepts of safety factor and the probability of failure. Let the capacity of the system be g_c (e.g., allowable strength) and the response be g_r. For the given vector **x** of input variables, the traditional safety factor is defined as the ratio of the capacity to the response, as

$$S(\mathbf{x}) = \frac{g_c(\mathbf{x})}{g_r(\mathbf{x})} \tag{13}$$

The system is considered to be failed when $S \le 1$ and safe when $S > 1$.

When the vector $\mathbf{x}$ of input variables is random, $g_c(\mathbf{x})$ and $g_r(\mathbf{x})$ are random in nature, resulting in the safety factor being a random function. In such instances, the safety of the system can be enforced by using the following reliability constraint:

$$P_f := \Pr(S(\mathbf{x}) \le 1) \le P_{f\,\text{target}}\,, \tag{14}$$

where P_f is the failure probability of the system and $P_{f\,\text{target}}$ is the target failure probability, which is the design requirement.

The last inequality in Eq. (14) can be converted into equality, if the upper bound of the safety factor is relaxed (in this case it is one). Let the relaxed upper bound be s^*. Then, the last part of the reliability constraint in Eq. (14) can be rewritten, as

$$\Pr(S(\mathbf{x}) \le s^*) = P_{f\,\text{target}}\,. \tag{15}$$

The relaxed upper bound s^* is called the Probabilistic Sufficient Factor (PSF). Using PSF, the goal is to find the value of PSF that makes the CDF of the safety factor equals to the target failure probability. Finding s^* requires inverse mapping of CDF, from which the terminology of inverse measure comes. A unique advantage of PSF is that design engineers, who are familiar to the deterministic design using the safety factor, can apply the similar notion to the probabilistic design

C. System Reliability Analysis

In the case of system reliability analysis, let there are k performance functions involved such that the system is failed when one of the performance functions is failed. Thus, the probability of failure is defined as the union of individual failure modes, as

$$P_f = \Pr[(y_1 \geq 0) \cup (y_2 \geq 0) \cup \cdots \cup (y_k \geq 0)]. \tag{16}$$

Then, the system performance function can be defined as

$$y_{\text{sys}} = \max\begin{pmatrix} y_1 & y_2 & \cdots & y_k \end{pmatrix}, \tag{17}$$

The function y_{sys} in Eq. (17) is a non-smooth function in general. Thus, the moment-based methods or response surface methods will be inaccurate. The system failure probability can be estimated using bounding technique[13], but for a complex system the bounds would be wide[14].

In the tail modeling, however, the cumulative distribution of the safety factor is estimated, in stead of y_{sys}. Thus the system PSF is defined as

$$S_{\text{sys}} = \min\begin{pmatrix} S_1 & S_2 & \cdots & S_k \end{pmatrix}, \tag{18}$$

Then, the same reliability constraint in Eq. (15) can be used by substituting S_{sys} into $S(\mathbf{x})$. The advantage of the system PSF is that all the output functions are automatically scaled into the safety factor.

IV. Numerical Examples

A. Beam Problem

The cantilever beam shown in Fig. 32 (Wu *et al.*[15]) is a commonly used demonstration example for reliability analysis and optimization. The length *L* of the beam is 100". The width and thickness is represented by *w* and *t*. It is subjected to end loads F_X and F_Y in the axial and transverse directions. The general design problem involves minimizing the weight or equivalently the cross sectional area: $A = w \cdot t$ subject to two reliability constraints, which require the failure probabilities to be lesser than a prescribed target failure probability. The two failure modes are expressed as two limit state functions:

Strength:
$$y_s = R - \sigma = R - \left(\frac{600}{w^2 t} F_X + \frac{600}{w t^2} F_Y\right) \tag{19}$$

Tip deflection:
$$y_d = D_O - D = D_O - \frac{4L^3}{Ewt}\sqrt{\left(\frac{F_Y}{t^2}\right)^2 + \left(\frac{F_X}{w^2}\right)^2} \tag{20}$$

where *R* is the yield strength, *E* is the elastic modulus, and *w* and *t* are the design parameters. *R*, F_X, F_Y, and *E* are random in nature and are defined in Table 1.

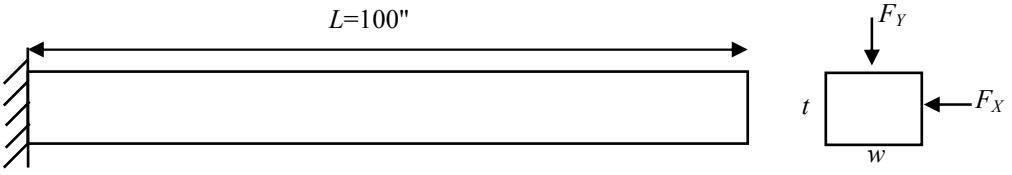

Figure 3. Cantilever beam subjected to horizontal and vertical random loads.

Table 1: Random variables for the cantilevered beam problem

Random Variable	F_X	F_Y	R	E
Distribution	Normal (500,100)lb	Normal (1000,100)lb	Normal (40000,2000) psi	Normal (29E6,1.45E6) psi

In this example, the discussion is limited to the estimation of failure probability in terms of PSF, with much less number of samples. Three different cases are discussed. Case 1 discusses the estimation of PSF for the strength failure mode using the tail modeling approach at different threshold values. Similarly the PSF estimation for the deflection failure mode is investigated in Case 2 and the system failure case where both the failure modes are considered simultaneously is discussed in Case 3. For all the cases, the convergence of PSF with respect to different thresholds and accuracy of PSF at different number of samples are investigated. Two methods, namely the maximum likelihood method and the least square regression method are used to estimate the parameters. The results from these methods are compared.

Case 1:

The first case considers the stress failure mode. The optimal values of the design variables w = 2.4526; t = 3.8884 for a target failure probability of 0.00135 are adopted from Qu and Haftka[16]. The corresponding value of PSF for this design is 1.0. 500 samples based on the distribution of the random variables are generated and the PSF is estimated for different thresholds as discussed in Section 2. This procedure is repeated 100 times and the mean, 5%, 95% confidence intervals are estimated. The results are presented in Figure 4.

It can be observed from Figure 4 that the PSF estimated by regression approach is very unstable whereas the median of PSF estimated by the ML approach is relatively stable. There is instability towards higher threshold like 0.98 but the corresponding exceedance data are very less, which explains the instability. The estimated mean of the PSF in the ML approach is close to 0.99 which is about 1% error in estimating the actual value of the PSF.

Case 2:

The deflection failure mode is addressed here. In the earlier case, the limit state function was linear. The limit state function for the deflection failure mode is a slightly nonlinear function in terms of x and y. The allowable deflection is chosen to be D_0=2.25. Similar to the stress failure case, the PSF is estimated at different thresholds for the optimal combination of the design variables. The results are presented in Figure 5.

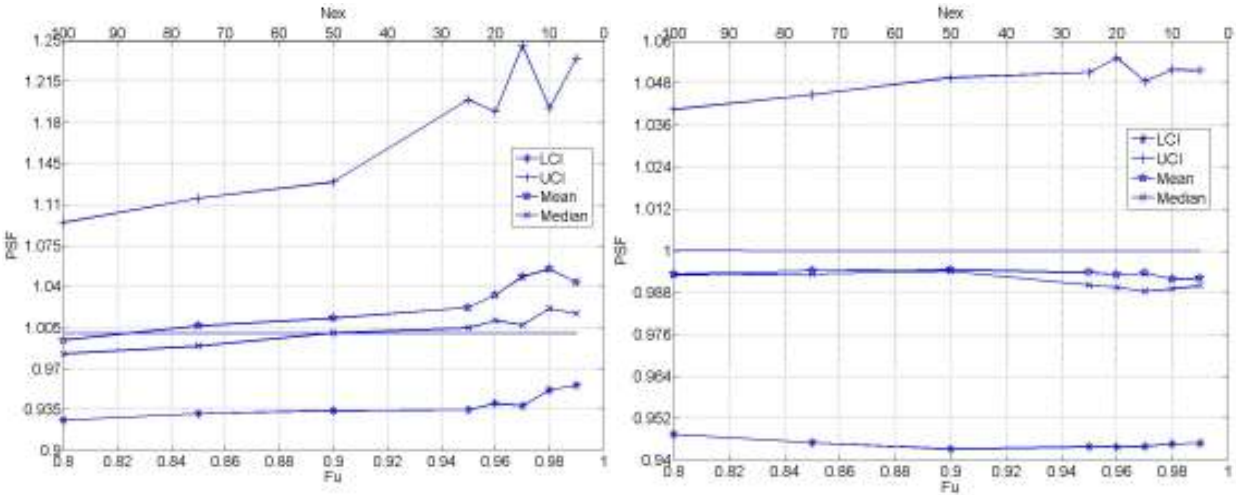

(a) Regression **(b) MLE**

Figure 4. Convergence of PSF at different thresholds for the stress failure mode. 500 Samples. 100 Simulations.

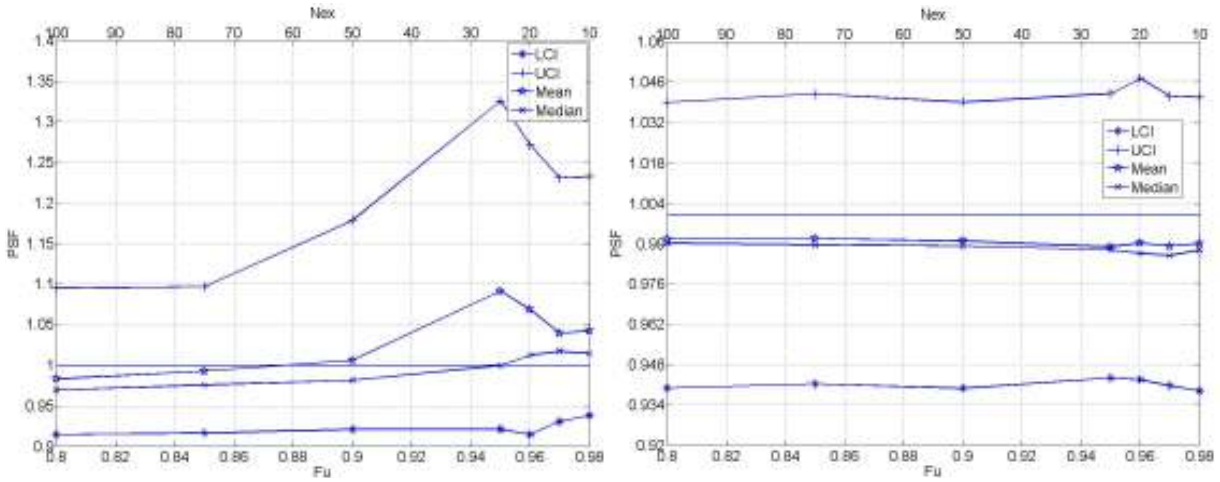

(a) Regression **(b) MLE**

Figure 5. Cantilever beam deflection failure mode. 500 Samples. 100 Simulations. Convergence of PSF at different thresholds.

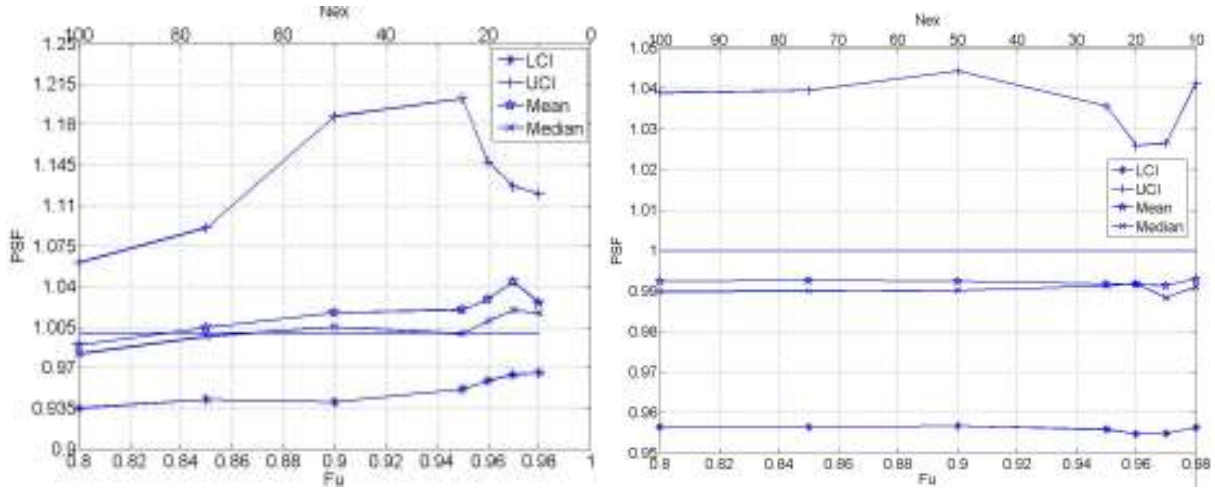

(a) Regression **(b) MLE**

Figure 6. Cantilever beam system failure mode. 500 Samples. 100 Simulations. Convergence of PSF at different thresholds.

Case 3:

Both the failure modes are considered simultaneously in this case. The safety factor for each failure mode is evaluated. For each realization, the critical of the two safety factor is considered the system safety factor. Once, the system safety factor is obtained for 100 simulations, the tail modeling approach is carried out and the corresponding system PSF is estimated. Here the design variables are w = 2.6041; t = 3.6746 and the allowable deflection D_0=2.145. This combination of the variables allows equal contribution of the modes to the total failure. The contribution of the modes are: P_{f1} = 0.00099; P_{f2} = 0.00117; $P_{f1} \cap P_{f2}$ = 0.00016. The convergence plots of PSF for the system failure case is presented in Figure 6. Figure 6 shows that the PSF estimated through parameters estimated by the regression method is unstable in contrast to the PSF estimated through parameters from the ML method. This behavior was observed in the other two cases too.

The number of samples used in the above studies is 500. The PSF is expected to converge to the actual value when the number of samples is increased. In order to understand the effect of number of samples on the PSF estimate, the convergence of PSF with respect to number of samples is studied for all the cases. The trend of convergence in all the cases was identical for both the methods. In order to avoid repetition, convergence plots for

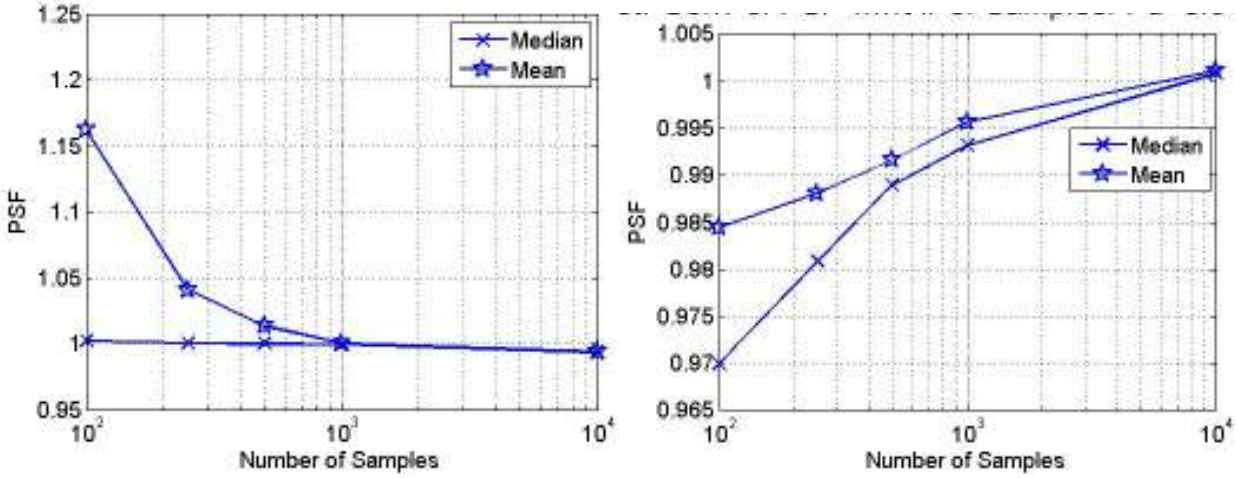

(a) Regression **(b) MLE**

Figure 7. Semilog plot. Cantilever beam system failure. Fu=0.90. Convergence of PSF at different number of samples. 100 Simulations at each number of samples.

the system case are alone presented in Figure 7. It is clearly depicted by the figure that there is essentially convergence in the accuracy of PSF as the number of samples is increased.

It is to be noted that in all the cases discussed, the accuracy of PSF at different thresholds were more or less uniform for the ML method. The mean excess plot was used as a tool to study effect of threshold and to choose the optimal threshold. The plot is presented in Figure 8. It can be clearly seen that the mean excess plot is almost linear for the entire range of the threshold values. This dictates the reason for the accuracy of PSF remaining stable at different thresholds. In this example, choosing a threshold as low as 0.70 also would have allowed us to estimate PSF with good accuracy.

From the above discussions, it can be concluded that the tail modeling approach using GPD to model the tails and estimating the failure probability therein is capable of modeling the tails of responses in structural applications adequately. It is possible to estimate PSF with an error of 1% with only 500 samples.

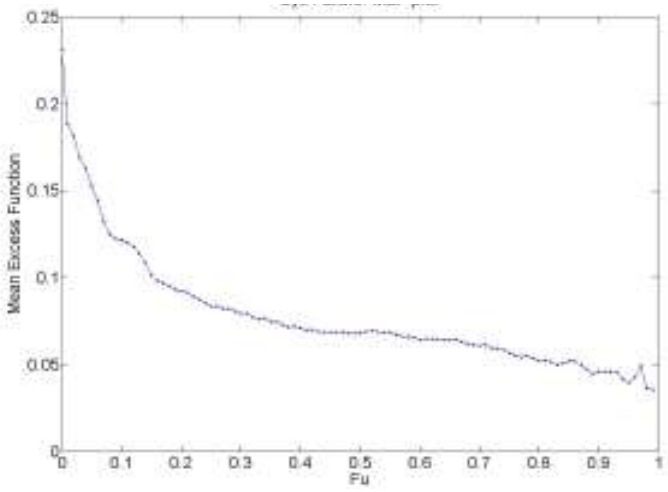

Figure 8. Cantilever beam system failure. Mean excess plot. 500 Samples.

B. Tuned Mass-Damper Example

The tail modeling approach to estimate the failure probability is demonstrated here with the help of a tuned mass damper example. The tuned mass damper problem in Figure 9 is taken from Chen *et al*.[17]. The problem involves the failure probability estimation of a damped single degree of freedom system with dynamic vibration absorber. Figure 9 illustrates the tuned damper system consisting of the single degree of freedom system and a dynamic vibration absorber to reduce the vibrations. The original system is

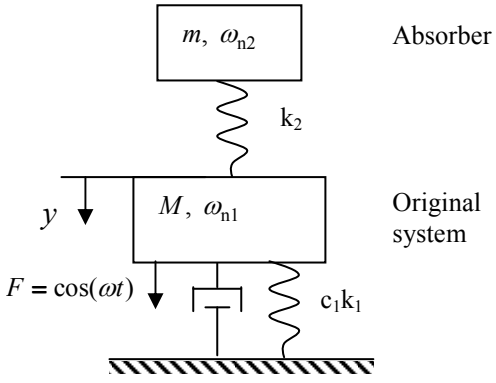

Figure 9. Tuned vibration absorber

externally excited by a harmonic force. The absorber serves to reduce the vibration. The amplitude of vibration depends on

1. $R = m/M$, the mass ratio of the absorber to the original system
2. ζ, the damping ratio of the original system
3. $\beta_1 = \omega_{n1}/\omega$, ratio of the natural frequency of the original system to the excitation frequency
4. $\beta_2 = \omega_{n2}/\omega$, ratio of the natural frequency of the absorber to the excitation frequency

The amplitude of the original system y is normalized by the amplitude of its quasi static response and is a function of four variables expressed as:

$$y = \frac{\left|1 - \left(\frac{1}{\beta_2}\right)^2\right|}{\sqrt{\left[1 - R\left(\frac{1}{\beta_1}\right)^2 - \left(\frac{1}{\beta_1}\right)^2 - \left(\frac{1}{\beta_2}\right)^2 + \frac{1}{\beta_1^2\beta_2^2}\right]^2 + 4\zeta^2\left[\left(\frac{1}{\beta_1}\right) - \frac{1}{\beta_1\beta_2^2}\right]^2}} \tag{21}$$

This example treats β_1 and β_2 as random variables. They follow a normal distribution N(1,0.025) and $R = 0.01$, ζ=0.01. The normalized amplitude of the original system is plotted in Figure 10. There are two peaks where the normalized amplitude reached undesirable vibration levels. The corresponding contour plot is presented in Figure 10. The failure region is denoted by the red band. This failure region is an island. That is, the failure region has safe regions on either side of it. This introduces additional challenges of not being able to use analytical approaches like FORM because the failure region is not a half plane. The objective of the problem is to reduce the risk of the normalized amplitude being larger than a certain value. The limit state for this case is expressed as:

$$g(\beta_1, \beta_2) = y(\beta_1, \beta_2) - y_0 \tag{22}$$

where y_0 can be considered as the allowable level of vibration. When the limit state in Eq. (22) is greater than 0, failure is said to occur. Increasing or decreasing y_0 will help in decreasing or increasing the failure probability respectively. y_0 = 27 is considered for the discussion. The corresponding failure probability with 1E5 sample MCS is estimated to be 0.0103. The tail modeling approach with 500 samples and 100 simulations are used to study the convergence and accuracy estimates of PSF. The plot for PSF at various thresholds is presented in Figure 11. From the plots, it seems that regression behaves better compared to the ML method. There is a discrepancy in the plot corresponding to the ML method. The PSF estimated at 0.96 threshold is accurate than the PSF estimate at a threshold of 0.98. In order to understand the behavior of the tail of the tuned mass damper, a log plot of the CDF with 1E5 samples is examined. The plot is presented in figure 12.

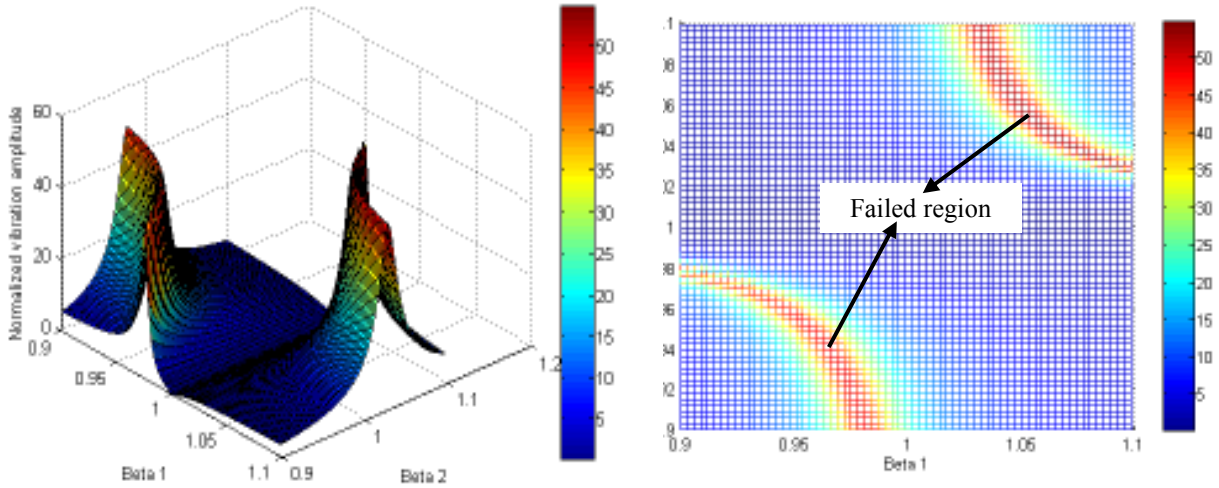

Figure 10: Normalized amplitude of vibration absorber with respect to β_1 and β_2

It is evident from the plot that there are two curvatures in the tail which are difficult to model. And, the GPD has to capture this shape with less exceedance data. This is the reason for the discrepancy in the ML plot, the shape of the tail at the area of interest (S=1) modeled by ML with a threshold of 0.96 was better than the tail model with a threshold of 0.98. In order to further explore the tail models from each method, the tail model from each method is superimposed on each other and the comparative plots are presented in Figure 13. It is clearly observed that the tail modeled based on ML approach denoted by the broken line attempts to capture the second curvature and in the process introduces error in the PSF value corresponding to a failure probability level of 0.01. On the other hand, the model obtained based on regression parameters represented by the solid line, approximates the tail in a linear fashion and is accurate compared to the tail based on ML method for a failure probability of 0.01. However, the ML method is expected to perform better when the failure probability to be estimated is low. When the failure probability is low, it becomes necessary to model the second curvature adequately to estimate the PSF with reasonable accuracy. The ML method can perform better than the regression approach in modeling the second curvature.

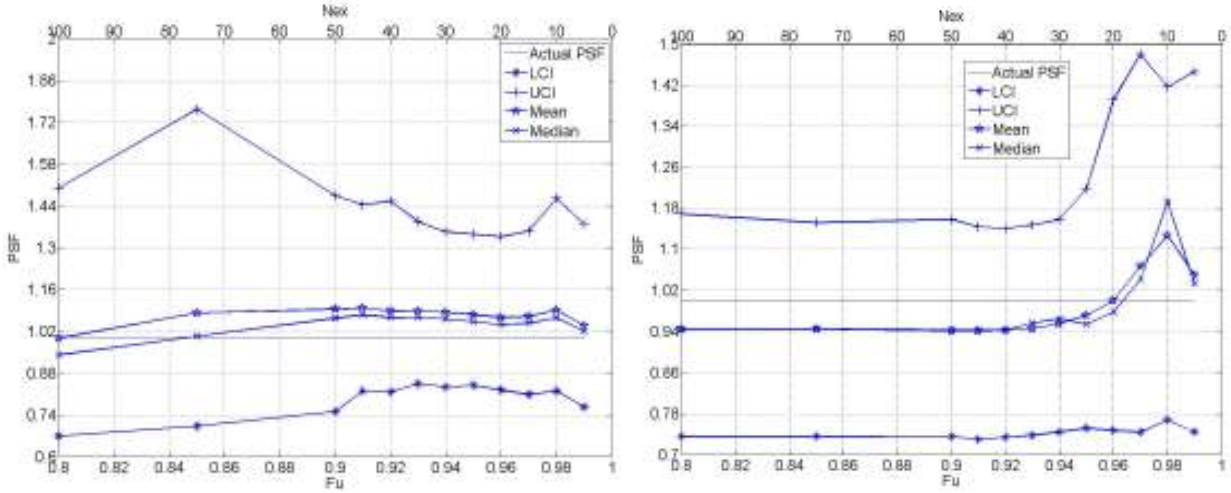

(a) Regression (b) MLE

Figure 11: Tuned Mass Damper. Convergence of PSF at different thresholds. 500 samples. 100 Simulations

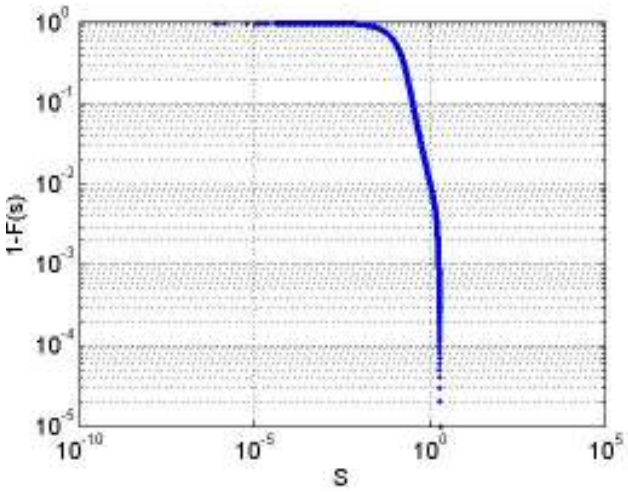

Figure 12: CDF of normalized amplitude. 1e5 Samples.

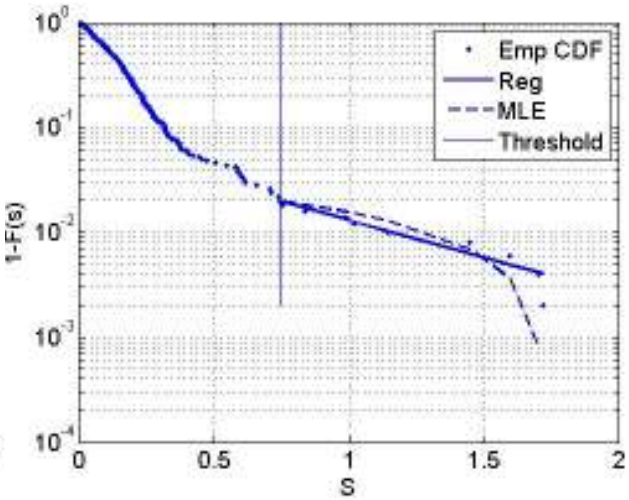

Figure 13: Comparison of tail models using regression and ML method.

This type of CDF might not be encountered in structural applications often and solving this problem with less number of samples is very challenging. It was shown that it is possible to estimate the PSF close to 1% error. With more insight on the problem, it is possible to select the suitable parameter estimation method depending on the requirements. Here, if one needs to estimate PSF corresponding to failure probabilities lesser than 1e-3, then the second curvature has to be modeled well and hence ML method is a good choice. Else, for higher failure probabilities, regression can perform better.

V. Conclusions

A tail modeling technique is utilized to estimate the system reliability with multiple modes of failure. The tail modeling allows focusing on the behavior of the tail with equivalent tail behavior. The generalized Pareto distribution provides a convenient tool for estimating high probability data with much less number of samplings than the conventional Monte Carlo simulation. The upper tail of the probabilistic sufficient factor is modeled using tail modeling, which allows a convenient way of modeling system failure mode. Two numerical examples show that the both regression and maximum likelihood function provide accurate estimation of parameters. The effect of threshold and the accuracy tail estimation are investigated in detail. When 500 samples are used, in the numerical examples, the accuracy of tail estimation was with thin 1% error.

References

[1]Maes, M., and Huyse, L. (1995), Tail effects of uncertainty models in QRA, Proceedings of the Third International Symposium on Uncertainty Modeling and Analysis, IEEE Computer Society Press, 133-138.

[2]Castillo, E. (1988), Extreme value theory in engineering, Academic Press, San Diego, California, USA.

[3]Pickands, J. III (1975), Statistical inference using extreme order statistics, Annals of Statistics, 3 119-131.

[4]Maes, M.A. and Breitung, K. (1993), Reliability-Based Tail Estimation, Proceedings, IUTAM Symposium on Probabilistic Structural Mechanics (Advances in Structural Reliability Methods), San Antonio, Texas, June, 335-346

[5]Boos, D. (1984), Using extreme value theory to estimate large percentiles, Technometrics, 26 (1) 33-39.

[6]Hasofer, A. (1996), Non-parametric estimation of failure probabilities, Mathematical Models for Structural Reliability, Eds. F. Casciati, and B. Roberts, CRC Press, Boca Raton, Florida, USA, 195-226.

[7]Caers, J., and Maes, M. (1998), Identifying tails, bounds, and end-points of random variables, Structural Safety, 20 1-23.

[8]Prescott, P., and Walden, A. (1980), Maximum likelihood estimation of the parameters of the generalized extreme-value distribution, Biometrika, 67 (3) 723-724.

[9]Hosking, J. (1985), Algorithm AS 215: Maximum-likelihood estimation of the parameters of the generalized extreme-value distribution, Applied Statistics, 34 (3) 301-310.

[10]Lee, J. O., Yang, Y. S., Ruy, W. S., A Comparative Study on Reliability-index and Target-performance-based Probabilistic Structural Design Optimization, Computers and Structures, Vol. 80, No. 3-4, 2002, pp. 257-269.

[11]Youn, B. D., Choi, K. K., and Park, Y. H., Hybrid Analysis Method for Reliability-based Design Optimization, Journal of Mechanical Design, ASME, Vol. 125, No. 2, 2003, pp. 221-232.

[12]Ramu, P., Qu, X., Youn, B.D., Haftka, R.T., Choi, K.K., Safety Factor and Inverse Reliability Measures, 45th AIAA/ASME/ASCE/AHS/ASC Structures, Structural Dynamics, and Materials Conference, Palm Springs, CA, April 2004 - paper AIAA-2004-1670.

[13]Cornell, C. A., Bounds on the reliability of structural systems, J. Struct. Div. ASCE, Vol. 93 (1), 1966,171-200.

[14]Ditlevsen, O., Narrow reliability bounds for structural systems, J. Struct. Mech, Vol. 7, 1979, 453-472.

[15]Wu, Y T., Shin Y., Sues, R., and Cesare, M., "Safety Factor Based Approach for Probability–based Design Optimization," Proceedings of 42nd AIAA/ ASME/ ASCE/AHS/ASC Structures, Structural Dynamics and Materials Conference, Seattle, WA, 2001, AIAA Paper 2001-1522.

[16]Qu, X., and Haftka, R. T., Reliability-based Design Optimization Using Probabilistic Sufficiency Factor, Journal of Structural and Multidisciplinary Optimization, Vol. 27, No.5, 2004, pp. 314-325.

[17]Chen, S., Nikolaidis, E. and Cudney, H. H., "Comparison of Probabilistic and Fuzzy Set Methods for Designing under Uncertainty", Proceedings, AIAA/ASME/ASCE/AHS/ASC Structures, Structural dynamics, and Materials Conference and Exhibit, 2860-2874, 1999.